

PROTON THERAPY MONTE CARLO SRNA-VOX CODE

by

Radovan D. ILIĆ

Vinča Institute of Nuclear Sciences, University of Belgrade, Belgrade, Serbia

Review paper
DOI: 10.2298/NTRP1204355I

The most powerful feature of the Monte Carlo method is the possibility of simulating all individual particle interactions in three dimensions and performing numerical experiments with a preset error. These facts were the motivation behind the development of a general-purpose Monte Carlo SRNA program for proton transport simulation in technical systems described by standard geometrical forms (plane, sphere, cone, cylinder, cube). Some of the possible applications of the SRNA program are: (a) a general code for proton transport modeling, (b) design of accelerator-driven systems, (c) simulation of proton scattering and degrading shapes and composition, (d) research on proton detectors; and (e) radiation protection at accelerator installations. This wide range of possible applications of the program demands the development of various versions of SRNA-VOX codes for proton transport modeling in voxelized geometries and has, finally, resulted in the ISTAR package for the calculation of deposited energy distribution in patients on the basis of CT data in radiotherapy. All of the said codes are capable of using 3-D proton sources with an arbitrary energy spectrum in an interval of 100 keV to 250 MeV.

Key words: Monte Carlo code, 3-D geometry, CT, patient anatomy, proton dose, therapy planning

INTRODUCTION

There is growing evidence that Monte Carlo-based programs are the most powerful tools in nuclear particle transport calculations. A number of medical physicists now believe that, in the near future, routine dose calculations will be performed by Monte Carlo methods [1, 2] and that these methods will serve as dominant vehicles for dose computation in radiotherapy treatment planning [2]. The most powerful feature of the Monte Carlo method is the possibility of simulating each of the individual particle interactions in 3-D and performing numerical experiments with a preset error. These facts were the motivation behind the development of a general-purpose Monte Carlo program, SRNA [3], for proton transport simulation in technical systems described by standard geometrical forms (plane, sphere, cone, cylinder, cube). Some of the possible applications of the SRNA program are: (a) a general code for proton transport modeling, (b) a design of accelerator-driven systems, (c) simulation of proton scattering and proton-degrading shapes and compositions, (d) research of proton detectors, and (e) radiation protection of accelerator installations. A wide range of possible applications of the program requires the development of SRNA-VOX [4] codes for

proton transport modeling in voxelized geometries and, finally, of the package ISTAR [5], for radiotherapy calculation of the deposited energy distribution in patients on the basis of CT data. All codes are capable of using 3-D proton sources with arbitrary energy spectra in the range of 100 keV to 250 MeV.

In the first part of this paper, a description of a common model of proton transport for both codes is presented. In the remainder of the paper, the results of numerical experiments performed by the SRNA code are compared with results of well-known GEANT [6] and PETRA [7] programs. In all instances, good agreement was demonstrated. The deposited energy distribution for a 65 MeV proton beam irradiating the patient's eye, calculated by SRNA-VOX, is presented in several CT slices. For the simulation of the therapeutic proton beam characterization by the multi-layer faraday cup (MLFC), at the Indiana University Cyclotron Facility (IUCF), the SRNA program was used [8]. An excellent coincidence between the measured and simulated results demonstrated the advantages of the MLFC as a measuring device. By adding the cross-section of positron emitter creation, the same program enabled the Brookhaven National Laboratory to simulate the spatial distribution of these emitters, which was a step preceding the estimation of proton dose distribution by positron emission tomography [9]. Depth-dose distribution profiles, as

* Author's e-mail: rasacale@gmail.com

well as vertical and horizontal dose profiles of the SRNA-VOX code, were obtained at the Proton Therapy Center of the Institute of Nuclear Research of the Russian Academy of Sciences, Troitck [10].

PROTON TRANSPORT MODEL

The simulation of proton transport is based on the multiple scattering theory of charged particles [11-13], energy losses with fluctuation [14, 15] and our model of compound nucleus decay simulation after proton absorption in inelastic nuclear interactions, as well as the Russian MSDM for compound nuclei and decay in SCHIELD-HIT [16].

Energy loss, proton step and energy scale

In order to simulate proton transport, the proton trajectory is divided into small steps whose length, Δs , is determined by the small energy loss ΔE

$$\Delta s = \frac{E_n}{E_{n-1}} \frac{dE}{(dE/dx)_{tot}} \quad (1)$$

The energy loss $\Delta E = E_n - E_{n+1}$ is chosen so as to equal several percentages of the initial proton energy. The conditions for the implementation of the multiple-scattering theory and calculation of energy loss due to fluctuation, demand that the energy scale be in part linear and, in part, logarithmic.

Energy E_{pek} , which splits the energy scale into linear and logarithmic parts, can be arbitrarily chosen.

From minimal energy E_{poc} to E_{pek} energy interval has logarithmic energy scale $E_1 = E_{poc}/(1/2)^{k_1}$, and from E_{pek} to E_{max} energy interval has linear energy scale with step $\Delta E_p = E_n - E_{n-1}$, where n is the last index in the logarithmic scale.

The model in the PTRAN program [17] shows that the best results are obtained with E_{pek} amounting to approx. 10 MeV. The volume and quality of energy and angular distributions are determined by the choice of the energy scale. To our experience, the best energy scale is obtained when the ΔE_{av} average energy loss is around $0.05 E_{pek}$.

After the energy scale is prepared, it is necessary to modify it. First, the average number of collisions at step Δs must be greater than the minimal value ($\Omega > 10$), according to the multiple-scattering theory. Secondly, Vavilov's parameter κ must be lesser than the maximal value ($\kappa < 20$). After several iterations, both conditions can be met and the energy scale prepared for the final calculation of proton transition probabilities. The stopping power (dE/dx) can be obtained from ICRU49 or calculated according to empirical Ziegler formulae [18].

Energy loss fluctuation

Usually, the probability density distribution and distribution functions are calculated in the following order: first the probability density function, upon which, the distribution function is calculated from the density function. The SRNA code uses another approach [19], namely that of calculating the distribution function directly. The starting point of our calculations is the function given by Vavilov in the following form

$$f(\Delta s, \Delta) = \frac{1}{\pi \xi} \kappa \exp[\kappa(1 - \beta^2 C)] \int_0^\infty \exp(\kappa f_1) \cos(y \lambda - \kappa f_2) dy \quad (2)$$

$$f_1 = \beta^2 [\ln y - Ci(y)] \cos y - y Si(y)$$

$$f_2 = y [\ln y - Ci(y)] \sin y - \beta^2 Si(y)$$

$$\kappa f_1 = \kappa f_1 - y^2 \frac{D}{\varepsilon_{max}}$$

Here $\lambda = (\Delta - \Delta_{av})/\xi$, λ_{av} denotes the distribution parameter, Δ – the probable energy loss, and Δ_{av} – the average energy loss. The remaining terms in (2) have the following meaning

$$\xi = 2\pi r_e^2 m_e c^2 \rho N_a \frac{\Delta s}{\beta^2} \sum_j w_j \frac{Z_j}{A_j} \quad (3)$$

$$\lambda_{av} = \frac{1}{\kappa} \frac{C \beta^2 \ln \kappa}{\xi}$$

$$\kappa = \frac{\xi}{\varepsilon_{max}}$$

$$\varepsilon_{max} = \frac{2m_e c^2 \beta^2}{1 - \beta^2} \frac{1}{(1 - 2m_e)/[M(1 - \beta^2)]} (m_e/M)$$

where ρ is the density, N_a – the Avogadro's number, r_e – the classical electron radius, m_e – the electron rest mass, M – the mass of the proton, Z_j , A_j , and w_j are atomic number, atomic weight, and weight fractions of the j^{th} constituent respectively, Δs – the proton step, $C = 0.5772156649\dots$ – the Euler's constant, ε_{max} – the maximum amount of energy a proton can lose with a free orbital electron, $Si(x)$ and $Ci(x)$ – the integral sine and cosine, and D – the Shulek's correction [14]

$$D = \frac{4}{3} \sum_n I_n g_n \ln \frac{2m_e c^2 \beta^2}{I_n} \quad (4)$$

for the influence of electron orbits on the distribution. In (4), I_n is the excitation potential of the electron orbit and g_n the ratio of the number of orbital electrons to the total number of electrons.

In order to calculate the distribution function, eq. (2), it should be first integrated over λ . In this manner, the obtained function is transformed into a form suitable for numerical integration by the Gauss-Kronrod algorithm. The choice of integration limits over y and step depends on the characteristics of the function. The quality of integration is estimated by the numerical parameters: absolute error equal to 10^{-7} ,

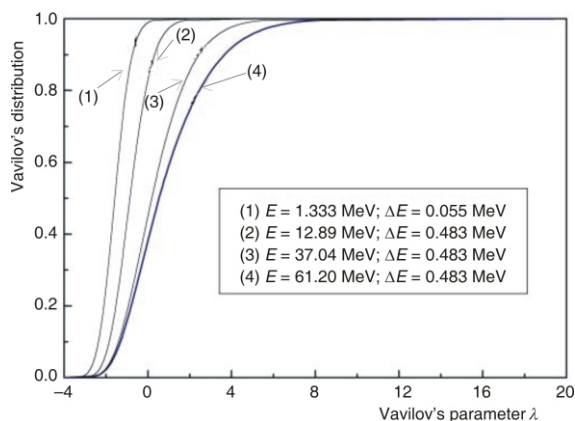


Figure 1. Vavilov's distribution of average energy loss in water

relative error equal to 10^{-6} , and distribution normalization onto 0.999999. Under these conditions, $y_{\max} = 100$ and take the values between -5 and 35 .

Vavilov's distribution obtained in this manner is shown in fig. 1. Shulek's correction has effect when higher atomic numbers cause the spreading of distribution. It is necessary to calculate at least 256 values of inverse distribution, using the cubic spline approximation.

Proton angular distribution

The angular distribution of multiple scattered protons was obtained by the integration of Molière's density function. This density function is derived in form of order [11, 12], with parameter $B - \ln(B) = \ln(\Omega)$, where Ω denotes the average number of collisions at step Δs

$$F(\vartheta) = \frac{1}{\chi_c \sqrt{B}} \int_0^{\vartheta} d\varphi \frac{f_n(\varphi)}{B^n} \varphi \quad (5)$$

In (5) $\vartheta / (\chi_c \sqrt{B})$ denotes the reduced angle and $f_n(\varphi)$ are Molière's functions given by

$$f_m(\varphi) = \frac{1}{m!} \int_0^{\infty} dy \frac{y^2}{4} \ln \frac{y^2}{4} J_0(\varphi y) \exp \frac{y^2}{4} \quad (6)$$

where $J_0(\varphi y)$ is the Bessel function. For compound materials, Molière's screening angle is given by

$$\chi_c = 4\pi N_a r_e \frac{m_e}{M} \frac{\tau}{\tau + 2} \sum_j w_j \frac{Z_j^2}{A_j} \Delta s \quad (7)$$

In (7), N_a denotes the Avogadro number, r_e and m_e – the classical radius and rest mass of the electron, M – the mass of the proton, $\tau = E_k / (Mc^2)$ – the reduced kinetic energy of the proton, w_j – the weight fraction of element Z_j and atomic weight A_j , and Δs – the proton step. We have calculated functions (6) in the interval $0 < \varphi < 40$ using the Gauss-Kronrod algorithm, once again. Inverse Molière distributions were calculated similarly to Vavilov's inverse distribution. Angular proton distributions for values of proton energy E are shown in fig. 2.

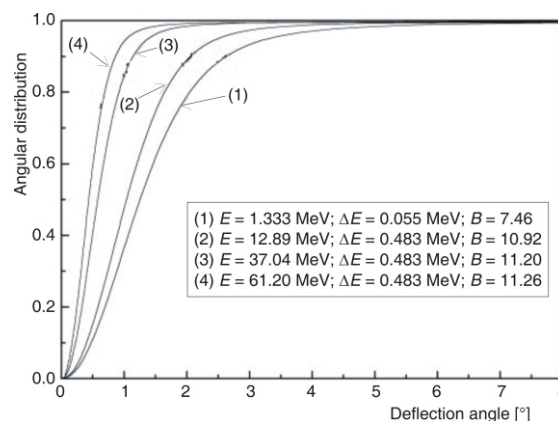


Figure 2. Angular distributions of multiple scattered protons in water

Inelastic nuclear interactions

Inelastic nuclear interactions are rare but, nevertheless, of great importance for the correct modeling of proton transport. In order to simulate inelastic nuclear interactions in materials, the cross-sections for all constitutive elements of these materials must be known. For a limited number of elements, these cross-sections are available in the energy range from the threshold up to 150 MeV [19], in ICRUTAB, up to 250 MeV [20, 21]. The SHIELD-HIT program uses the Russian multi-stage dynamical model (MSDM) generator of inelastic nuclear interactions MSDM. It includes all versions of SRNA. According to current trends in the development of treatment-planning tools based on Monte Carlo techniques, we can expect an expansion of such cross-section data.

With the data available, we have managed to establish a model of inelastic nuclear reaction simulations and secondary particle emissions. The model comprises following steps: (1) determination of the occurrence of the inelastic reaction event, (2) selection of the nucleus that the proton interacts with and the energy transferred to the nucleus, (3) probable number of secondary particles, and (4) energy and angle of the secondary particles emitted. For each of the steps, distributions described are needed.

Average number of inelastic nuclear interactions

The average number of interactions at proton step Δs is calculated according to the following relation

$$q(E) = \rho \frac{N_a}{A} \int_{E_n}^{E_n + \Delta E} \sigma(E) \frac{dE}{(dE/dx)} \quad (8)$$

where ρ is the density, $\sigma(E)$ – the inelastic nuclear interaction cross-section, and (dE/dx) – the total stopping power. Figure 3 shows the average number of inelastic nuclear interactions with the proton in ^{16}O .

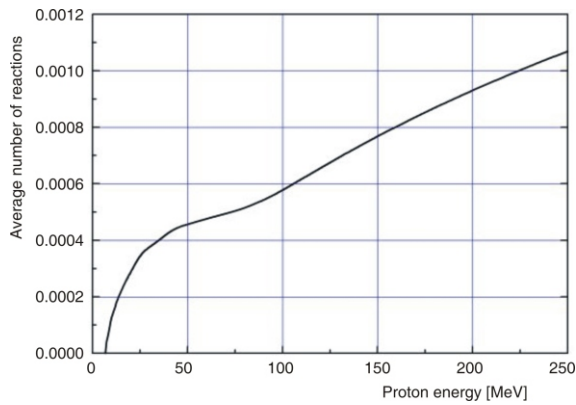


Figure 3. The average number of inelastic proton interactions in ^{16}O

Probable nucleus and recoil energy

The probable interaction of nucleus j with a proton will result in an inelastic nuclear reaction that is determined by the cumulative distribution $P_j = \sum_{i=1}^j p_i$, where $p_i = g_i \sigma_i / \sum_{k=1}^m g_k \sigma_k$ are the probabilities for nucleus i whose weight contribution equals g_i ; m is the total number of nuclei within the material. ICRUTAB data contains the values of recoil energy E_{ric} per inelastic nuclear reaction of the proton with the nucleus. If the energy of the proton is E_p before a reaction, then the created compound nucleus occurs with an energy of $E_p - E_{\text{ric}}$, while the energy E_{ric} is deposited at the site of the reaction.

Energy and angle of secondary particles

When the compound nucleus is created, according to Chadwick's model, it will decay by the simultaneous emission of neutrons, protons, deuterons, tritons, alpha-particles, and photons. For each single particle emitted, a mean multiplication factor F_m exists in the ICRUTAB data. If we accept that in cases as rare as this the Poisson distribution is adequate, we can determine the probable number of particles emitted for each single type of particle. Such a model demands that, for each single type, the probable number of secondary particles must be found even when F_m is of a very small magnitude. Our model of compound nucleus decay simulation comprises all possible combinations of emission of all six of the secondary particles and proton energies mentioned above. A separate preparation of transition probabilities for the emission of secondary particles, which works in SRNADAT, is not necessary when applying the Russian MSDM generator of inelastic nuclear interactions. SRNA code includes transport as an alternative to the MSDM generator of inelastic nuclear interactions. The MSDM generator describes all stages of the nuclear inelastic nuclear reaction and secondary particles emission: n ,

p , d , t , H_e^3 and alpha particles, including their numbers, energy and emission angle. In the SRNA transport simulation model, only secondary protons are included, while deuterons, tritons and alpha particles are deposited on the spot. Neutrons and photons are not included into this transport model. They are registered in the data file, where each line contains: the index of the particle, energy, (x, y, z) -co-ordinates, sine and cosine of polar and azimuth angles. This data file may be used by the MCNP program [22] in order to simulate neutron and photon transport or by FOTELP programs [23-26] and PENELOPE [27], for the simulation of photon transport, only.

Change of proton position and direction

At the end of each proton step, the direction of the proton is changed. The change of direction is specified in terms of polar ϑ and azimuth φ angles, in a co-ordinate system whose polar axis coincides with the direction of the motion of the proton at the beginning of the step. The polar angle is sampled from Molière's distribution, the azimuthal angle from a uniform distribution in 2π . The co-ordinates of a proton from a local to a fixed co-ordinate system are given by the Euler transformation. The coordinates of the proton after passing step Δs in the fixed co-ordinate system are given by

$$\begin{aligned} \Delta x &= \Delta s \sin(\vartheta) \cos(\varphi) \\ \Delta y &= \Delta s \sin(\vartheta) \sin(\varphi) \\ \Delta z &= \Delta s \cos(\vartheta) \end{aligned} \quad (9)$$

where ϑ and φ are the polar and azimuthal angles.

Place of event over the step

At step Δs , the proton can lose energy ΔE or be absorbed by inelastic nuclear interactions. The density functions of the position of such events are unknown. We have supposed a uniform distribution of such events. This is more realistic than the usual assumption that they take place at the end of a proton step.

Cross-border between zones

The length of proton step Δs_m is calculated in advance, according to the material in question. In some cases, the length of the proton step can be larger than distance L to the zone border, calculated in the direction of proton transport. In the nearest material itself, the proton step and other condensed history proton parameters exhibit different values. Because of this, an attempt focused on solving the problems at the borderline between the two zones in the easiest possible manner, without increasing the simulation time or signifi-

cant perturbations of the physical processes involved, have been made. In SRNA codes, the energy lost, ΔE_m , over step Δs_m , was multiplied by the factor $L/\Delta s_m$, so as to get the energy deposited in the current zone, if only that of $L < \Delta s_m$. After that, proton starting point has been moving onto zone border. The deflection angle is sampled from the appropriate, previously prepared distribution (5).

Random number generators

From the multitude of available random number generator programs, we have used the DALARAN/LAPACK routine (version 2.0), developed by the University of Tennessee, University of California, Berkeley, NAG Ltd., Courant Institute, Argonne National Laboratory and Rice University 1992. This program routine provides a random real number from a uniform (0,1) distribution, using the multiplicative congruential method with modulus 2^{48} . As an alternative, SRNA can use the Matsumoto and Nishimura generator for generating uniform pseudorandom numbers with the biggest 2^{19917} period.

Geometry

Particle transport simulation is limited by the geometrical description of the transport medium. The real geometrical shapes of technical systems can be described by planes and second-order surfaces, as in PENGEO from PENELOPE, MCNP, RFG [28] that include programs for 2-D and 3-D visualization. For describing patient geometry, standard shapes are usually applied. This is only a crude approximation, because it is a version of the technical description of patient geometry. The most accurate way of describing patient geometry is by means of CT data [29]. CT data permit 3-D transport simulation, including the variation of tissue densities and compositions. Using the same proton transport model, we have developed two versions of the SRNA program. The first version of our code uses RFG or PENGEO (from PENELOPE) programs as geometrical modules. The second, voxelized version, is adjusted to the use of CT data and GEMVOX, with our routine heightened speed calculation to estimate the distance from the position of the proton inside the voxel to its nearest plane.

Conversion of Hounsfield's number to density

The dimensions and number of voxels, along with the Hounsfield number, are the basis for the preparation of simulation data. The main problems of determining the density and elemental composition of patient tissue on the basis of CT data are described

here. In our model, in order to spare computer memory, the intervals of the Hounsfield number are associated with elemental tissue composition and its density.

With the help of the DICOM standard, we were able to distinguish Hounsfield's numbers and to convert them into an integer matrix $MH(i, j, k)$, where (i, j, k) are the indices of the voxel. Their contents, presented on the screen, enable us to select, in as-possible-as natural way, the types of tissue that surround a tumor, as well as the Hounsfield numbers that correspond to them. In tissues selected in such a manner, we join the density and limits around the mean values of the Hounsfield number from the (H_L, H_{L+1}) interval. Using this approach, the data in tab. 1 were created. For better simulation, the preparation of CT parameters is reduced to the conversion of the density of each voxel to the matrix $MG_n(i, j, k) = 10000\rho_n[MH(i, j, k)]$ for each single tissue (material) from L to N . Without repetition, we have managed to enable transition probabilities and other constants necessary for the simulation of all materials of interest. Each of the materials gets its identification, $10000\rho_n$, by which we recognize the type of material constituting the voxel. Then, with the help of anatomical pictures, we have found that for the same tissue material, we have come up with different Hounsfield numbers and that these tissues have retained their natural elementary structure and density. In cases such as these, our program treats the same materials of different densities as different materials.

Proton sources

In SRNA codes, proton sources are in the form of beams of circular and rectangular cross sections. The beams can be rotated in 4π around the irradiated object. For the purpose of accelerator simulations, it is possible to obtain phase-space files of particles on the reference surface. These files, produced by the SRNA code, contain proton energy, position and direction data in each of the lines and can be used as proton sources.

Installations for the production of proton beams are spatially and geometrically complex. The part of the installation which is used to adjust the beam to the tumor has a number of elements through which the protons that enter the tumor receive the desired spectrum. To meet these requirements SRNA-VOX has routines that prepare the output file with the states of protons that reach the selected surface of the irradiated tissue. For all 3-D simulations of the dose delivered to the tumor ISTAR proton source includes the possibility of modulating the beam energy by passing through an appropriate degrade energy as well as to modulate the intensity and the direction of the beam.

Table 1. Intervals of the Hounsfield number with average densities and tissue composition, according to available data given by Schneider *et al.*: *Mat* – tissue; *H_{nd}* – Hounsfield number, *r* – density [*gcm⁻³*]

<i>Mat</i>	<i>H_{nd}</i>	<i>r</i>	<i>H</i>	<i>C</i>	<i>N</i>	<i>O</i>	<i>P</i>	<i>C_a</i>
1	-950	Air						
2	-741	0.26	10.3	10.5	3.1	74.3	0.2	
3	-98	0.93	11.6	68.1	0.2	19.8		
4	-77	0.95	11.4	59.8	0.7	27.8		
5	-55	0.97	11.2	51.7	1.3	35.5		
6	-49	0.98	11.5	64.4	0.7	23.1		
7	-22	1.00	11.0	52.9	2.1	33.5	0.1	
8	-1	1.02	10.6	33.2	3.0	52.8	0.1	
9	11	1.03	10.5	41.4	3.4	43.9	0.1	
10	23	1.03	10.6	11.5	2.2	75.1	0.1	0.5
11	42	1.05	10.4	11.9	2.4	74.5	0.1	0.7
12	102	1.10	9.6	9.9	2.2	74.4	2.2	
13	385	1.25	7.8	31.6	3.7	43.8	4.0	8.5
14	466	1.30	7.3	26.5	3.6	47.3	4.8	9.8
15	586	1.36	6.9	36.6	2.7	34.7	5.9	12.8
16	657	1.41	6.4	26.3	3.9	43.6	6.0	13.1
17	742	1.46	6.0	25.0	3.9	43.5	6.6	14.3
18	843	1.52	5.6	23.5	4.0	43.4	7.2	15.6
19	999	1.61	5.0	21.2	4.0	43.5	8.1	17.6
20	1113	1.68	4.6	19.9	4.1	43.5	8.6	18.7
21	1500	1.75	4.2	20.4	3.8	41.5	9.3	20.2

The number of protons from the source determines the final accuracy of simulation results. In cases of middle and low density tissue irradiation, more than 10^9 proton histories are needed. For the random number generators implemented on 32-bit computers, 10^9 is approximately the maximal amount of the uncorrelated numbers that can be provided. The SRNA program can simulate a source with a higher numbers of protons than the restrictions prescribe. These sequences of simulation conditions correspond to the central limit theorem on the basis that it determines accuracy. When the requested accuracy is achieved in a part of the tumor, all relevant data and the required number of protons from previous simulations are applied to the next simulation. Rather than being a source of the integer, the actual number of protons is divided into a large number of sequences so that, after the conversion to a whole number of protons, SRNA can perform the requested simulation. This problem is not present when using 64 bit computers.

Scoring grid and precision of simulation

In both versions of the SRNA code, a grid of rectangular elemental volumes for energy deposition scoring [MeVkg^{-1}] is used. If CT data are applied to the simulation, the grid is coincident with that of CT voxels. On the other hand, the same grid is also used for the precise determination of energy deposition. Our SRNA code calculates the precision of simulations for each material zone or appropriate separate

parts of these zones. It permits us to carry out a precise estimation of the deposited energy x_i with regards to each elemental volume or groups of volumes. During the simulation, the values of x_i and x_i^2 are scored for each voxel or groups of elemental volumes. At the end of the simulation, precision is calculated using the said two obtained values. The variance of the population of x values is a measure of the spread within these values and the i is given in formulae $\sigma^2 = E(x) [E(x)]^2$. The square root of variance σ is the so-called standard deviation of population scores. As with $E(x)$, σ is seldom known, but can be estimated by Monte Carlo as S , given by

$$S^2 = \frac{1}{N} \sum_{i=1}^N (x_i - \bar{x})^2$$

The details of the application of the cited formula are omitted in literature, while label N is used to treat a full range of summations of the random size. A specific feature of the SRNA as well as the PENELOPE code is the usage of series of proton batches that allows correct application of the Central Limit Theorem for assessing accuracy.

NUMERICAL EXPERIMENTS AND MEASUREMENTS

Due to the limitations of cross section data for inelastic nuclear interactions and available simulation data obtained by other codes, our numerical experiments pertain to water and tissue. The results of these numerical experiments for initial proton energies, in the energy interval from 25 to 250 MeV, are presented here.

Interesting numerical experiments have been carried out utilizing the SRNA code in connection to the use of the Multi-Layer Faraday Cup for the measurement of proton beam energy spectra. The results of the distribution of the proton absorbed dose in the human eye simulated by the SRNA code were published at the Bologna QUADOS 2003 Intercomparison [30]. The feasibility of positron emission tomography of dose distribution in proton beam cancer therapy was investigated at the Brookhaven National Laboratory, using a modified SRNA-2KG code. Proton depth-dose distribution, vertical and horizontal dose profiles in water measurement and simulation by the SRNA code performed at the Institute for Nuclear Research, Russian Academy of Sciences, are in good agreement. These results are subsequently described in detail. The most interesting numerical experiments with protons were performed in voxelized geometry using patient CT data.

Homogeneous phantom

The homogeneous phantom, usually water or tissue equivalent, is dominated by the measurements of the spatial dose distribution of protons and unduly modest in simulations of other materials. For the verification of this model of proton transport, it was necessary to compare the results of simulations and measurements. The results of the SRNA-2KG code for the homogeneous water phantom are compared with the results of PETRA and GEANT codes from our model and PETRA models in treating inelastic nuclear interactions. When, in the SRNA code, the transport of secondary protons is excluded, the results of PETRA and PTRAN are coincident with our results. The results of the full model are shown in fig. 4 for 26.4 MeV proton energy in a homogeneous water phantom.

The real picture of deposited energy changes along the depth and arrow of the Bragg peak requires a low-energy cutoff. For this reason, the cutoff energy in SRNA codes is nominally set to less than 1 MeV, depending on the proton energy input. This result is shown in fig. 5. The maximum of the Bragg peak ap-

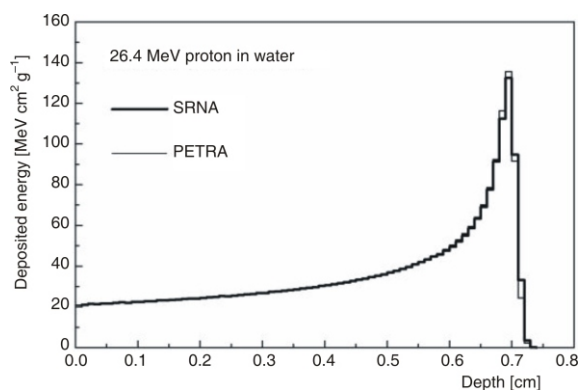


Figure 4. Monte Carlo simulation of depth-dose distribution in water for 26.4 MeV proton beams

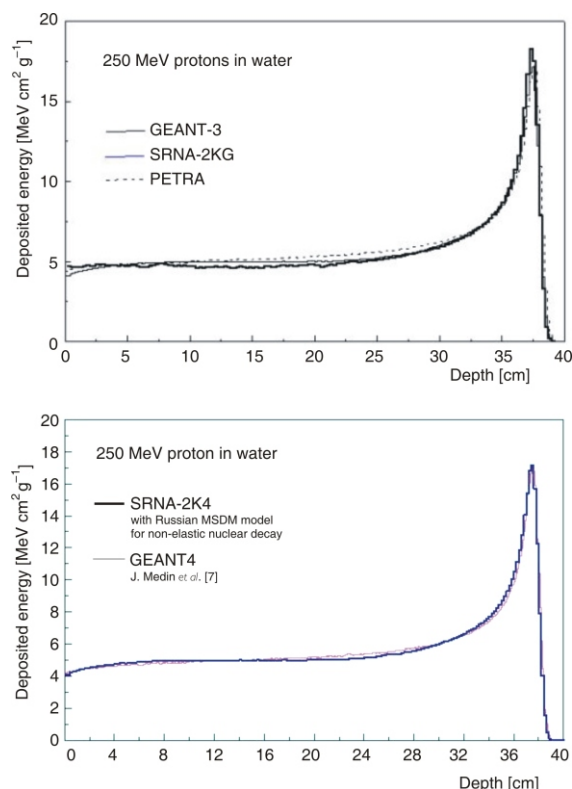


Figure 5. Monte Carlo simulation of depth-dose distribution in water for 250 MeV proton beams

pears at a depth that agrees with the theoretical proton range. It shows that the model of proton passage is correct. At energies less than 100 MeV, the influence of inelastic nuclear interactions is small, hence their effect is not visible. As pointed out previously, these reactions, although rare, have a significant influence on the deposited energy distribution. Their increasing influence can be seen in fig. 5, where the results for proton beam energy of 250 MeV in a water phantom, obtained by SRNA-2KG, SRNA-2K4, GEANT, and PETRA codes, are presented. These results illustrate the applicability of our code for higher proton energies. It should be mentioned that the variations of curves for shallower depths in fig. 5 are a result of compound nucleus decay. With the increase in depth, this effect decreases, due to an increase in ionization losses.

Multi-layer Faraday cup experiments

The quality and reproducibility of the proton beam is of great importance in proton therapy. In order to achieve the desired dosimetric precision, the beam must be calibrated with respect to the predetermined initial energy and acceptable energy spread. At the Indiana University Cyclotron Facility, a multi-layered Faraday cup (MLFC) was used to characterize the proton beam of the accelerator. In this project, the Monte Carlo simulation, using SRIM, SRNA-2KG and

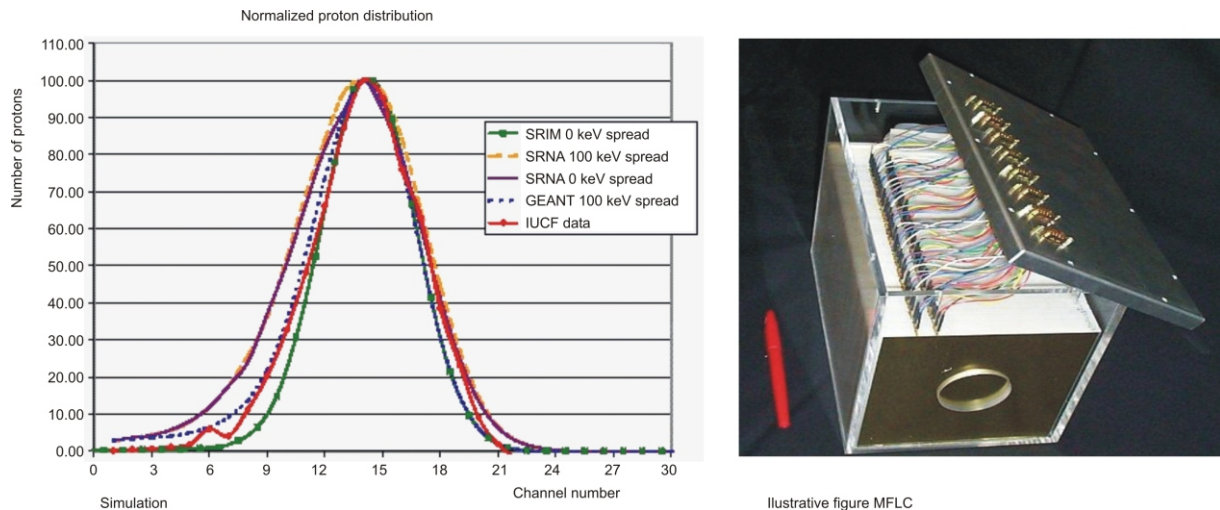


Figure 6. Number of protons stopped simulated by Monte Carlo simulation, measured by the multi-layered Faraday cup with a 205 MeV proton beam

GEANT3 codes, provided data which were then compared with the actual measurement data. MFLC counts the number of protons stopping in each of its many conducting layers by measuring the proton current of each layer. Figure 6 shows the simulated and measured data for 205 MeV proton energy with different spreads. The MFLC will resolve energy spreads in order of 900 keV, proving useful in determining the initial beam energy to within 100 keV.

Absorbed dose in human eye proton therapy

The European Commission and Italian ENEA have, with the support of OECD, organized an intercomparison workshop of computational tools used in radiation dosimetry (QUADOS), because of the importance of quality control of computational tools used in radiation dosimetry. The expertise of numerical dosimetry is applied to health physics and clinical dosimetry studies, defined by special agreements with other institutions and hospitals included in the project. ENEA has always upheld the opinion that numerical dosimetry and Monte Carlo techniques should play a key role in dosimetry and radiation protection. The programs included in the said intercomparison project were: MCNP 2.4 (Los Alamos National Laboratory), MARS 14 (FermiLab), SRNA (Vinča Institute of Nuclear Sciences), and FLUKA 2002 (Politecnico di Milano). Within the project, the benchmark case -problem No P3 has set up the calculation of the deposited dose from two proton beams: the first one being 50 MeV monoenergetic, while the second one with specific energy spectrum of a spread-out bragg peak within the range from 40 MeV to 50 MeV [30]. The proton

beam is easily obtained with a small accelerator. In these conditions, using the SRNA-VOX with voxel dimensions 0.5 cm 0.5 cm 0.5 cm, we get a result with a statistical error better than 1.5% for the model of the human eye, as shown in fig. 7 and for the spectrum of protons in fig. 8.

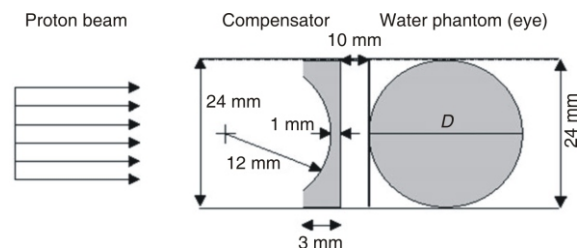


Figure 7. QUADOS model of human eye

Inhomogeneous and voxelized geometries

Preliminary results obtained by the SRNA code are the basis of our attempt to simulate proton dose distribution in real patient geometry by using CT data with pixel dimensions equaling 0.81 cm 0.81 cm and slice thickness of 0.5 cm. We have supposed that some tumors lie in the eye base. In simulation, this kind of eye tumor was irradiated with a 65 MeV proton beam with a circular cross-section with a radius of 1.2 cm. This simulation is performed with 100000 incident protons and tissue data pertaining to the 21 "materials" from tab. 1. Deposited energy distributions in patient slices, obtained by the SRNA code, are presented in fig. 9.

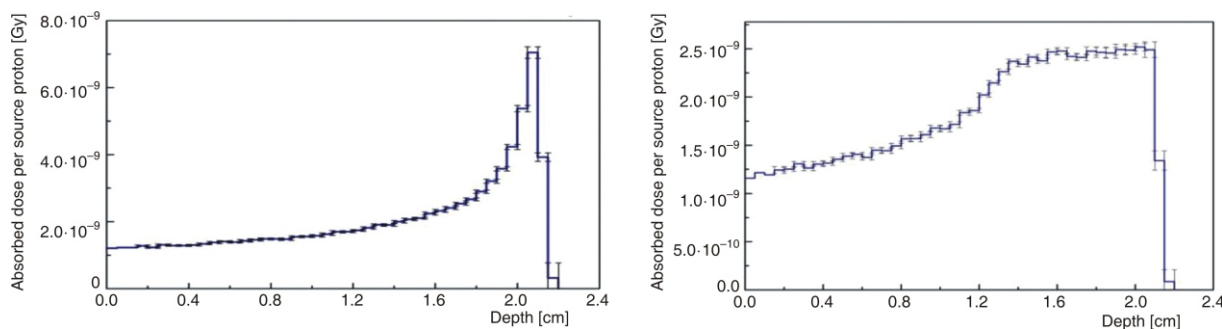


Figure 8. Proton depth-dose distribution in human eye model; 50 MeV proton beam energy (left); from 40 MeV to 50 MeV proton spectrum (right)

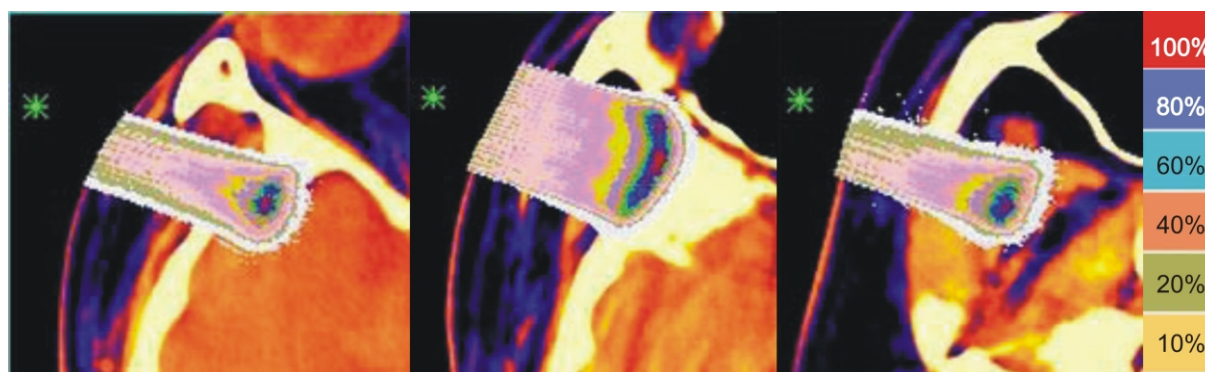


Figure 9. Deposited energy in eye slices normalized at maximum values of each slice obtained by the SRNA code by voxelized geometry on the basis of CT data and tissue data from tab. 1

Positron emitter distribution simulation

During proton therapy, positron emitters are created in the tissue (for instance, ^{11}C , ^{13}N , ^{15}O) in inelastic nuclear interactions. The verification of the therapy can be achieved by comparing the PET image descending the positron activity distribution with the predicted target dose distribution used to plan the treatment? For feasibility estimation purposes, at the Brookhaven National Laboratory, the SRNA-2KG program was modified by the inclusion of positron emitter cross-sections, and then, their spatial distribution within the tissue was simulated at a 250 MeV proton beam with a 2 mm diameter as illustrated in fig. 10.

Absorbed dose distribution of the INR proton beam

The vertical and horizontal depth-dose distribution in water was measured on proton beams at the Institute of Nuclear Research of the Russian Academy of Sciences (fig. 11) and simulated by the Monte Carlo technique using SRNA and TRIM codes with voxels sized 5 mm 5 mm 5 mm [27]. The initial proton energy equaled 158.6 MeV. Depth-dose distribution was measured by an IC-10 chamber and diamond detector.

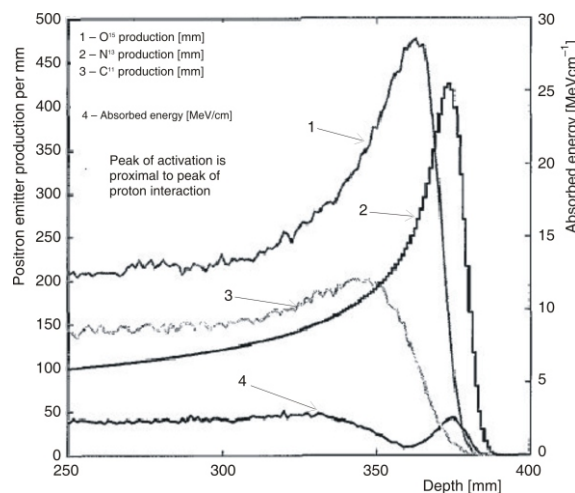


Figure 10. Positron emitter production per mm and depth-absorbed energy in MeV/cm

The Bragg peak coincided within a margin of mm, the measured proton range was 163 mm and mean proton energy equaled 153.0 MeV. This is very close to the SRNA-simulated value of 153.3 MeV. The measured horizontal and vertical dose profiles were in reasonable or good agreement with the simulated data.

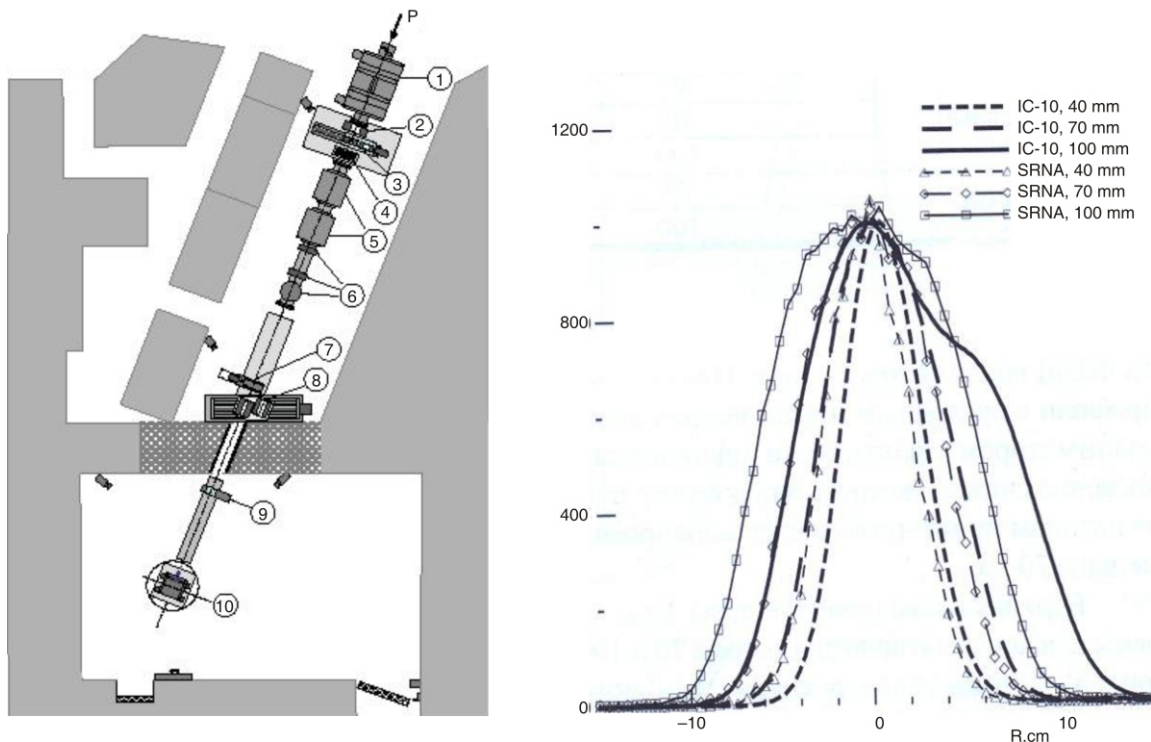


Figure 11. Cross-section of the INR (Troitzk, Russia) proton beam

P – proton from linac; 1 – Al foil 1 mm; 2, 3 – collimators 40, 70, and 100 mm in diameter; 4 – emergency shutdown; 5 – kapton foil, 0.15 mm; 6 – vertical magnet; 7 – second collimators; 8 – shield (left) and vertical and horizontal dose profiles in an arbitrary unit (right)

ISTAR – proton dose planning software

For the past few years, the attention of medical physicists has focused on possible applications of Monte Carlo techniques in radiotherapy planning in general and, more specifically, proton therapy. In clinical practice, available anatomy imaging techniques are nearing the desirable geometric resolution for the definition of tumor shapes and dimensions, necessary for therapy planning. Such trends lead to the solution of two important problems of proton therapy planning: (1) the development of a Monte Carlo proton transport numerical engine capable of producing a therapy plan in acceptable time and, (2) development of on-line clinical procedures comprising all steps necessary for proper patient treatment. The capabilities of ISTAR software in solving the first of the two problems are presented next.

It is assumed that the location of the tumor is defined with sufficient precision by the CT image. Irradiation planning begins with the selection of the tumor region within a rectangular box. The selected region is defined by the indices of the first and last CT slice in the longitudinal (Z) direction and by marking the area in the transversal (X-Y) plane. The position of the beam center, defining the position of the proton beam axis, should be selected at this step.

Following this, a database User Set for proton beams (mean energy and type of distribution, direction

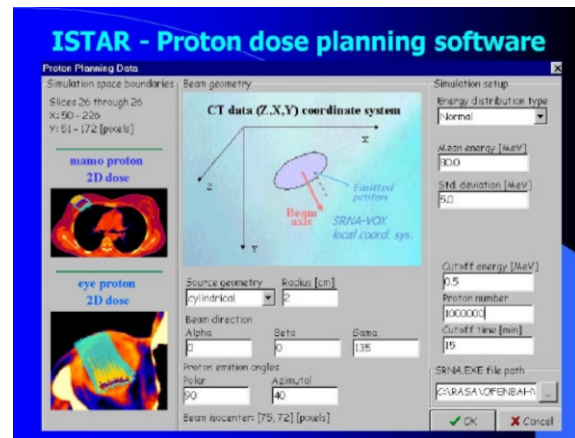


Figure 12. View of the proton dose planning menu

of emission, circular or square cross-sections of the beam, number of protons needed for the database, etc. are devised, as shown in fig. 12.

Using transition probabilities for all tissue types presented in tab. 1, prepared in advance with the SRNADAT code and the files created by ISTAR, the Monte Carlo simulation starts the execution of the SRNA-VOX code. Using the said data, as well as the Srna.inp file and the Hound.dat file, (converted from the Hound.txt for the actual tissue material), the simulation of the proton transport begins. After the simulation is completed, several useful output files are avail-

able. Redose.txt contains the number of slices and X/Y axis pixels, followed by the values of the absorbed dose in each voxel. After returning to ISTAR, the values of the absorbed proton dose are displayed over the CT slice image. These values can be normalized, either to the maximum value in a single slice or to the maximal value over the entire irradiated region. Image-viewing commands include transparency (blending) intensity control. The code also allows the selection of different palettes for the display of various isodose levels. The capabilities of the ISTAR proton dose planning software cover the following two examples: the eye uveal melanoma and that of breast tumor.

Eye dose distribution

The CT of the patient's head with voxel dimensions of 0.5 cm 0.045 cm 0.045 cm was used. The melanoma was assumed to be at the bottom of the eye, spherically shaped, with a radius of 0.8 cm. Using ISTAR software, a therapy plan was made using a 1 cm radius of a cylindrical proton beam with a mean energy of 50 MeV and a Gaussian energy spectrum with a spread of 1.2 MeV. The simulation was performed with 10^6 proton histories. Figure 13 shows the proton dose distribution on a slice in the equatorial plane of the eye.

Breast dose distribution

As a second example, a CT image of a breast with voxel dimensions of 0.5 cm 0.0732 cm 0.0732 cm was chosen. A therapy plan with a cylindrical proton beam of a 1.2 cm radius and Gaussian energy spectrum

($E = 65$ MeV, energy spread 1.2 MeV), and 10^6 protons in the beam is presented. The resulting proton dose distribution is displayed in fig. 13.

CONCLUSIONS

A model of the Monte Carlo SRNA code is described here, alongside representative numerical experiments. The results of these experiments, in good agreement with the results of several well-known codes, show the validity of the SRNA model of proton transport simulation. In the energy range of up to 26.4 MeV, inelastic nuclear interactions may be neglected; in the range of up to 66 MeV, the mentioned reactions should be considered for further rigorous simulation, while above 66 MeV, inelastic nuclear interactions must be included into the simulation. Numerical experiments by the SRNA, GEANT, SHIELD-HIT, and PETRA codes and measurements with the MLFC at IUCF, Indiana, USA, and INR, RAN, Troitck, Russia, show that our code is a very good and simple tool for testing the nuclear interaction model and that each Monte Carlo code to be used in charged particle therapy should pass these tests. These experiments prove the correctness of programs used in the SRNA Monte Carlo model for proton transport simulations with energies from 0.1 MeV to 250 MeV. According to existing trends in the development of therapy planning tools based on the Monte Carlo technique, we can expect the expansion of cross section data. The developed ISTAR software engine and included numerical illustrations show the feasibility of the use of our software in clinical practice.

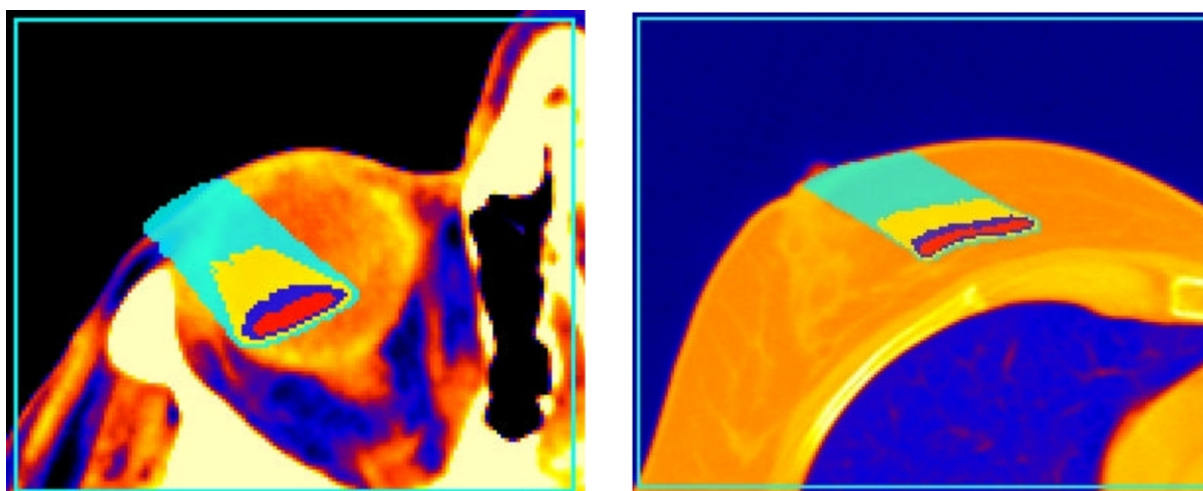


Figure 13. Dose distribution, equatorial eye plane, simulated by the SRNA-VOX code using 50 MeV protons with a 1.2 MeV energy spread; the isodoses equal values of 20%, 60%, 80%, and 100 % of the dose maximum (left); Dose distribution in mammography of the central beam plane simulated by the SRNA-VOX code using 65 MeV protons with a 1.5 MeV energy spread; the isodoses equal the values of 20%, 60%, 80 and 100 % of the dose maximum (right)

ACKNOWLEDGEMENTS

The development of SRNA codes has been supported by the TESLA Accelerator Installation, Department of Physics (010), and the Department of Radiation and Environmental Protection, Vinča Institute of Nuclear Sciences. We would like to thank J. Medin for his help in simulations by GEANT and PETRA and comparisons of the obtained results. Many thanks, as well, to colleagues: N. Schreuder from IUCF, Indiana University, J. J. Beebe-Wang from the Brookhaven National Laboratory, and V. N. Vasiliev, from the Institute of Nuclear Research, Russian Academy of Sciences, for their co-operation in simulations of SRNA code versions and measurements carried out in their laboratories.

REFERENCES

- [1] Sempau, J., Wilderman, S. J., Bielajew, A. F., DPM, A Fast, Accurate Monte Carlo Code Optimized for Photon and Electron Radiotherapy Treatment Planning Dose, *Phys. Med. Biol.*, 45 (2000), pp. 2263-2291
- [2] Hartmann Siantar, C. L., *et al.*, Lawrence Livermore National Laboratory's PEREGRINETM Project, *Proceedings*, 12th Conference on the Use of Computers in Radiotherapy, Madison, Wis., USA, *Medical Physics Publ.*, 1997
- [3] Ilić, R. D., Lalić, D., Stanković, S. J., SRNA – Monte Carlo Codes for Proton Transport Simulation in Combined and Voxelized Geometry, *Nucl Technol Radiat*, 17 (2002), 1-2, pp. 27-36
- [4] Ilić, R. D., *et al.*, The Monte Carlo SRNA-VOX Code for 3-D Proton Dose Distribution in Voxelized Geometry Using CT Data, *Phys. Med. Biol.*, 50 (2005), 5, pp. 1011-1017
- [5] Ilić, R. D., *et al.*, The Monte Carlo SRNA Code as the Engine in ISTAR Proton Dose Planning Software for the TESLA Accelerator Installation, *Nucl Technol Radiat*, 19 (2004) 2, pp. 30-35
- [6] ***, GEANT4 CERN Program Library Long Writup W5013
- [7] Medin, J., Andreo, P., PETRA – A Monte Carlo Code for the Simulation of Proton and Electron in Water, Internal Report MSF 1997-1, Karolinska Institutet, Stockholm University, Stockholm, 1997
- [8] Mascia, A., Schreuder, N. I., Ilić, R. D., Characterizing a Proton Therapy Beam with MultiLayered Faraday Cup, (2001)
<http://www.eps.rg/meet/HAW01/baps/abs/S40058.html>
- [9] Beebe-Wang, J. J., *et al.*, Feasibility of Positron Emission Tomography of Dose Distribution in Proton-Beam Cancer Therapy, EPAC, 2002, Paris
- [10] Vasiliev, V. N., *et al.*, Parameters and Absorbed Dose Distribution for the INR Proton Beam (in Russian), *Medicinskaya Fizika*, 43 (2009) 3, pp. 21-29
- [11] Berger, M. J., Monte Carlo Calculation of the Penetration and Diffusion of Fast Charged Particles, *Accad. Press, New York, USA, Methods in Computational Physics*, 1 (1963), pp. 135-215
- [12] Moliere, G., Theorie der Streuung schneller geladener Teilchen II: Mehrfach – und Vielfachstreuung. *Z. Naturforsch* 3a (1948), pp. 78-97
- [14] Vavilov, P. V., On the Ionizational Losses of High Energy Heavy Particles by Ionization, *J. of Phys. USSR*, 8 (1944), 4, pp. 201-205
- [15] Shulek, P., *et al.*, Fluctuation of Ionization Losses (in Russian), *Yadernaya Fizika*, 4 (1966) 3, pp. 564-566
- [16] Sobolevsky, N. M., SHIELD-HIT Monte Carlo for Simulating Interactions of High Energy Hadron with Complex Macroscopic Target, IAEA-1287, 2002
- [17] Berger, M. J., Proton Monte Carlo Transport Program PTRAN, Report NISTIR-5113, 1993
- [18] ***, ICRU Report 49 Stopping Power and Ranges for Protons and Alpha Particles, Bethesda, Md., USA, 1993
- [19] Ilić, R. D., Vavilov's Distribution Data Preparation for Heavy Charged Particles Transport by Monte Carlo (in Serbian), XLIII Conf. ETRAN, 1998, 20-22 September, Zlatibor, Serbia
- [20] Chadwick, M. B., Data ICRUTAB.TAR, 1998
- [21] Young, P. G., Chadwick, M. B., Neutron and Proton-Induced Nuclear Data Libraries to 150 MeV for Accelerator-Driven Application, Int. Conf. on Nucl. Data for Sci. and Technology, May 19-24, Trieste, Italy, 1997
- [22] Briesmeister, J. J., MCNP – A General Monte Carlo N-Particle Transport Code, Version 4B LA12625-M Los Alamos National Laboratory, N. Mex., USA, 1997
- [23] Ilić, R. D., FOTELP – Monte Carlo Transport of Photons, Electrons and Positrons; RSICC Computer Code Collection CCC-581, 1998
- [24] Ljubenov, V., *et al.*, Total Reflection Coefficients of Low Energy Photons Presented as Universal Functions, *Nucl Technol Radiat*, 25 (2010), 2, pp. 100-106
- [25] Stanković, S. J., *et al.*, Monte Carlo Analysis of the Influence of Different Packaging on MOSFET Energy Response to X-Rays and Gamma Radiation, *Acta Physica Polonica A*, 122 (2012), 4, pp. 655-658
- [26] Ljubenov, V. I., Simović, R. D., Universal Dependence of the Total Number Albedo of Photons on the Mean Number of Photon Scattering, *Nucl Technol Radiat*, 26 (2011), 3, pp. 249-253
- [27] Salvat, F., Fernandes-Vera, J. M., Sempau, J., PENELOPE – A Code System for Monte Carlo Simulation of Electron and Photon Transport NEA Data Bank, OECD, 2003
- [28] Altiparmakov, D. V., Beličev, P., An Efficiency Study of the R-Function Method Applied as Solid Modeler for Monte Carlo Calculations, *Progres in Nucl. Energy*, 24 (1990), 1-3, pp. 77-88
- [29] Schneider, W., Bortfeld, T., Schlegel, W., Correlation between CT Numbers and Tissue Parameters Needed for Monte Carlo Simulation of Clinical Dose Distribution, *Phys. Med. Biol.*, 45 (2000), 2, pp. 459-478
- [30] ***, QUADOS – Intercomparison on the Usage of Computational Codes in Radiation Dosimetry, *Proceedings*, Bologna, Italy, International Workshop, July 14-16, 2003

Received on June 12, 2012

Accepted on November 26, 2012

Радован Д. ИЛИЋ

МОНТЕ КАРЛО ПРОГРАМ SRNA-VOX ЗА ПРОТОНСКУ ТЕРАПИЈУ

Најмоћнија карактеристика Монте Карло методе је могућност симулације сваке појединачне интеракције честица у три димензије и могућност да се нумерички експеримент обави са унапред задатом грешком. Ове чињенице су биле мотивација за развој Монте Карло програма опште намене SRNA за симулацију транспорта протона у техничким системима описаним стандардним геометријским облицима (равни, сфера, купа, ваљак, коцка). Неке од области примене програма SRNA су: (а) општи програм за моделовање протонског транспорта, (б) развој система вођених акцелераторима, (в) симулација протонског расејања и деградација облика и композиција, (г) истраживање детектора протона и (д) заштита од зрачења акцелераторске инсталације. Широко поље примене овог програма захтевало је развој верзије програма SRNA-VOX за моделовање транспорта протона у вокселизованој геометрији, и на крају развој пакета ISTAR за планирање протонске терапије и прорачун просторне расподеле депоноване енергије у пацијенту на основу СТ података. Сви програми су способни да користе тродимензионалне изворе протона са произвољним енергетским спектром у опсегу од 100 keV до 250 MeV. Приказани су резултати компарације нумеричких експеримената ових програма са познатим програмима: GEANT, MCNP, PTRAN, PETRA и резултати изведених експеримената у водећим лабораторијама у свету: Брукхевен националној лабораторији (BNL), Циклотронској инсталацији Индијана универзитета (IUCF) и Институту за нуклеарна истраживања Руске академије наука (INR RAS). Овим је показано да верзије програма SRNA омогућавају развој пакета за примену протонске терапије у клиничкој пракси.

Кључне речи: Монте Карло програм, 3-D геометрија, СТ анализија пацијената, протонска доза, планирање терапије
